A Combined Approach of Using an SDBR and a STATCOM to Enhance the Stability of a Wind Farm

S. M. Muyeen, *Senior Member, IEEE*

***Abstract*—This paper presents a method to enhance the stability of a grid-connected wind farm composed of a fixed-speed wind turbine generator system (WTGS) using a combination of a small series dynamic braking resistor (SDBR) and static synchronous compensator (STATCOM). The SDBR and STATCOM have active and reactive power control abilities, respectively, and a combination of these units paves the way to stabilize well the fixed-speed wind farm. In this paper, a centralized control scheme of using an SDBR and a STATCOM together is focused, which can be easily integrated with a wind farm. Different types of symmetrical and unsymmetrical faults are considered to evaluate the transient performance of the proposed control scheme, applicable to a grid-connected wind farm. The effect of a multimass drive train of a fixed-speed WTGS in fault analysis, along with its importance in determining the size of the SDBR to augment the transient stability of a wind farm, is investigated. Extensive simulation analyses are performed to determine the approximate sizes of both SDBR and STATCOM units. Dynamic analysis is performed using real wind speed data. A salient feature of this work is that the effectiveness of the proposed system to minimize the blade–shaft torsional oscillation of a fixed-speed WTGS is also analyzed. Simulation results show that a combination of a small SDBR and STATCOM is an effective means to stabilize the wind farm composed of a fixed-speed WTGS.**

***Index Terms*—Induction generator, SDBR, stability, STATCOM, torsional oscillation, wind farm.**

I. Introduction

THE industry worldwide is turning increasingly to renewable sources of energy to generate electricity. Wind is the fastest growing and most widely utilized of the emerging renewable energy technologies in electricity systems at present, with a total of 194.4 GW installed worldwide at the end of 2010 [1]. Variable-speed wind turbine generator systems (WTGS) are getting more attraction than the fixed speed nowadays. However, fixed-speed WTGS technologies still retain a sizeable share on the wind power market due to their superior characteristics such as brushless and rugged construction, low cost, maintenance free, and operational simplicity. The lifetime of a wind turbine is expected to be more than 20 years. Therefore, it is still a matter of interest to investigate the interaction of a fixed-speed WTGS with a power system [2].

The fixed-speed WTGS that uses an induction machine as a wind generator has the stability problem similar to a synchronous generator (SG) [3]–[6]. This study focuses on both transient and dynamic stability improvement issues of the fixed-speed WTGS. Due to the huge penetration of wind power to the grid, wind farm grid codes have been developed recently in many countries in which fault ride through (FRT) is an important constraint to adopt with [7]–[11].

There are different techniques and compensating tools reported in power system literatures to augment the stability of the fixed-speed WTGS [6], [12]–[32]. Energy capacitor systems [12], [13], battery energy storage systems [14]–[16], superconducting magnetic energy storage systems [17]–[19], and flywheel energy storage systems [20] are very effective tools as having both active and reactive power control abilities. A static synchronous compensator (STATCOM) is also found to be a potential candidate to stabilize a fixed-speed WTGS [21]–[23]. The transient response of a pitch controller is comparatively slow, as reported in [24] and [25], compared with the flexible alternating current transmission system (FACTS) devices used in [12]–[23]. In addition to these, a dynamic braking resistor (DBR) can be used for wind generator stabilization [26]–[32]. As the DBR has only the active power control ability, it is good idea to incorporate a reactive power compensating device along with the DBR. For stability augmentation of a fixed-speed WTGS, a series DBR (SDBR) [29]–[31] is more effective than a DBR with a shunt-connected topology [26]–[28]. In [29] and [30], a simulation analysis is performed using only one fixed-speed WTGS that connects the grid. That study is symmetrical to a distributed topology where each SDBR is connected close to the individual wind generators and differs significantly from the centralized topology using only one SDBR installed at the wind farm terminal. Incorporation of an SDBR with a dynamic voltage restorer increases the system cost due to the presence of a transformer and an LC filter [31]. In earlier works with the SDBR [29]–[31], the effect of other SGs that exist in a realistic power system is not evident. This study focuses on transient and dynamic stability augmentation of a grid-connected wind farm composed of fixed-speed WTGSs using a combination of an SDBR and a STATCOM, the purpose of which lies to reduce the overall cost of the compensating devices.

Therefore, centralized SDBR and STATCOM are considered to be connected at the terminal of a wind farm that connects the power system to observe the effectiveness of the proposed system during normal and grid fault conditions, in this study. Instead of a representative wind farm model used in [29] and [30], where the components are expressed using a simple transfer function, realistic component modeling is considered in this study using the laboratory standard power system software package PSCAD/EMTDC [33]. The detailed six-mass drive

Manuscript received January 20, 2013; revised December 6, 2013.
The author is with the Renewable Energy Laboratory, Electrical Engineering Department, The Petroleum Institute, Abu Dhabi, UAE (e-mail: s.m.muyeen@ieee.org).
Digital Object Identifier 10.1109/JSYST.2013.2297180

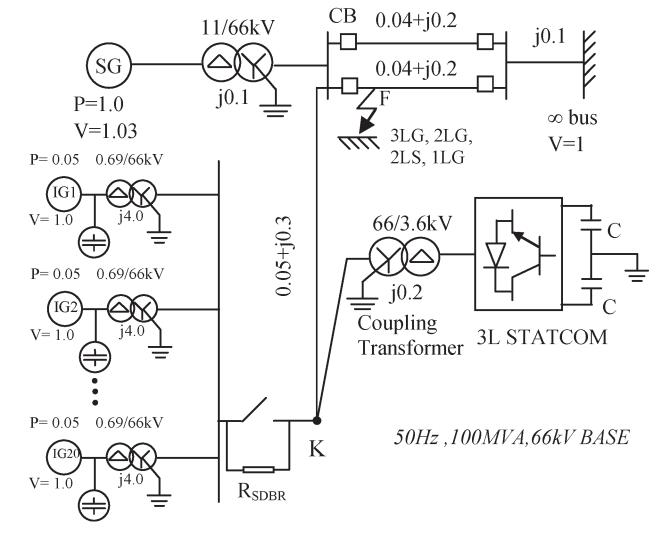

Fig. 1. Model system.

TABLE I
GENERATOR PARAMETERS

SG		IG	
MVA	100	MVA	2.5
Ra (pu)	0.003	r1 (pu)	0.01
Xa (pu)	0.13	x1 (pu)	0.1
Xd (pu)	1.2	Xmu (pu)	3.5
Xq (pu)	0.7	r21 (pu)	0.035
Xd′ (pu)	0.3	x21 (pu)	0.030
Xq′ (pu)	0.22	r22 (pu)	0.014
Xd″ (pu)	0.22	x22 (pu)	0.098
Xq″ (pu)	0.25	H (sec)	3.3
Tdo′ (sec)	5.0		
Tdo″ (sec)	0.04		
Tqo″ (sec)	0.05		
H (sec)	2.5		

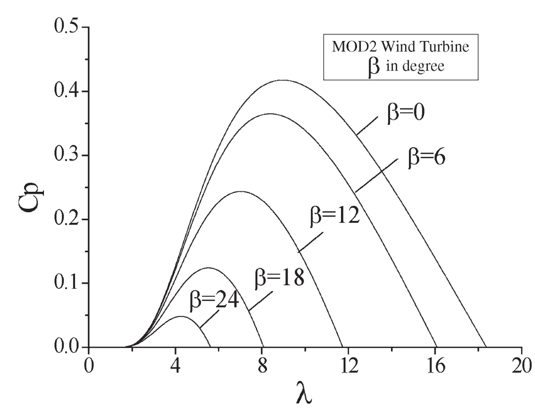

Fig. 2. $C_P - \lambda$ curves for different pitch angles.

train model is considered in a fixed-speed WTGS for the sake of precise analysis. The effect of a multimass drive train of a fixed-speed WTGS for fault analysis and its importance in determining the size of an SDBR unit that sufficiently augments the FRT capability of a wind farm are investigated in detail.

Power generation using wind energy deals with systems from engineering and science disciplines, e.g., mechanical, electrical, electronics, computer, and aerospace engineering. This study particularly focuses on two electrical systems, i.e., SDBR and STATCOM, including their control aspects to improve the stability of a wind energy conversion system along with the improvement of turbine blade–shaft torsional damping. Therefore, the study is essentially important for researchers working in systems-level and systems engineering.

To determine the minimum size required for both SDBR and STATCOM units to withstand against grid fault and to maintain constant terminal voltage during randomly varying wind speed condition, extensive simulation studies are performed. Real wind speed data measured in Hokkaido Island, Japan, are used in the dynamic analysis. Both symmetrical and unsymmetrical faults are considered as network disturbances in the analysis. One of the novel features of the study is that the effect of blade–shaft torsional oscillations of a fixed-speed WTGS during grid fault is analyzed, and it is reported how much the oscillation can be minimized using the determined small size of the SDBR and STATCOM. It is also reported how much the proposed scheme can enhance the stability of an SG available in the power system. Simulation results show that the proposed scheme, which combines small SDBR and STATCOM units, can enhance the transient and dynamic stabilities of a wind farm composed of fixed-speed WTGSs, as well as the entire power system.

II. Model System

Fig. 1 shows a model system used for the simulation analyses. One SG representing the main power plant is connected to an infinite bus through transformers and transmission lines, respectively. Twenty wind generators in a wind farm are connected to the grid through an individual transformer and a common transmission line. A capacitor bank C has been used for reactive power compensation of each induction generator IG at steady state. The value of capacitor C is chosen so that the power factor of the wind generator during the rated operation becomes unity [6]. The automatic voltage regulator and Governor (GOV) control system models for the SG used in this study are available in [6]. Generator parameters are shown in Table I. A centrally controlled SDBR is considered to be connected at a wind farm terminal. The STATCOM is connected to point K in Fig. 1. The system base power is 100 MVA.

III. Modeling of a Wind Turbine

A mathematical relation for mechanical power extraction from the wind can be expressed as follows [34]:

$$P_w = 0.5\rho\pi R^2 V_w^3 C_P(\lambda, \beta) \quad (1)$$

where P_w is the extracted power from the wind, ρ is the air density (kg/m^3), R is the blade radius (m), V_w is the wind speed (m/s), and C_p is the power coefficient, which is a function of both tip speed ratio λ and blade pitch angle β (deg). The wind turbine characteristic used in this study is shown in Fig. 2 for different values of β [35]. In this paper, the conventional pitch controller is considered in the simulation [34].

In this paper, the six-mass drive train model is considered for the precise analysis of a WTGS, as shown in Fig. 3, the details

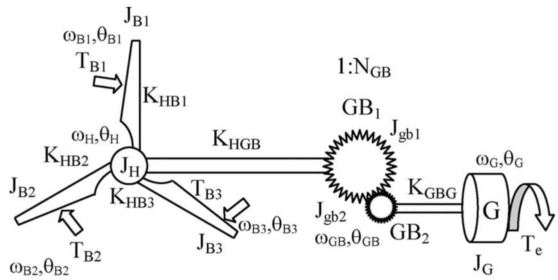

Fig. 3. Six-mass drive train WTGS.

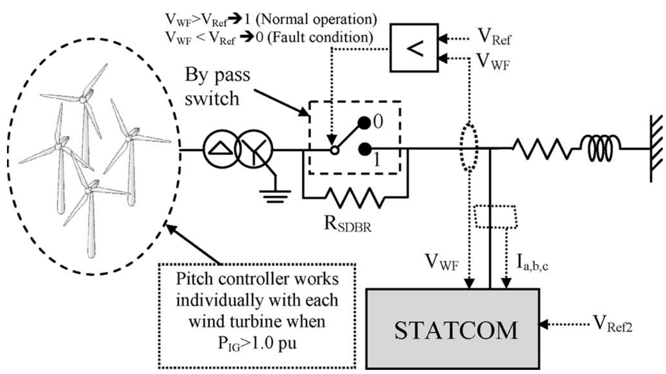

Fig. 4. Proposed coordinated control scheme for a wind farm.

of which are available in [6] and [36]. The parameters used in this study are given in the Appendix. Due to the high and low stiffness of the high- and low-speed shafts of the wind turbine, the torsional oscillation analysis of a wind turbine drive train is important.

IV. Modeling and Control Scheme

In this paper, a coordinated control scheme is adopted among the SDBR, STATCOM, and pitch controller to stabilize the wind farm under dynamic and network fault conditions. The coordinated control scheme is schematically shown in Fig. 4.

1) In normal operation, the wind farm terminal voltage deviates a lot due to the rapid wind speed fluctuations as the capacitor banks placed at the terminals of individual wind generators are designed to maintain a unity power factor under rated power conditions when the wind speeds are at rated values. The STATCOM will work during normal operation to maintain constant voltage at the wind farm terminal, and hence, the terminal voltage is set as the control input of the STATCOM in the coordinated control scheme. The STATCOM will also work during the grid fault condition when the terminal voltage falls below a threshold value.
2) The SDBR works only during the grid fault condition along with the STATCOM to enhance the FRT capability of the wind farm when the terminal voltage falls below the threshold value.
3) The pitch controllers are attached with individual wind generators and activate when the power exceeds the rated values of the generators. Therefore, wind generator output power is set as the input of the pitch controller. During the grid fault condition, the pitch controller will also activate when the wind generator power exceeds the rated values, particularly when the fault occurs at high wind conditions.

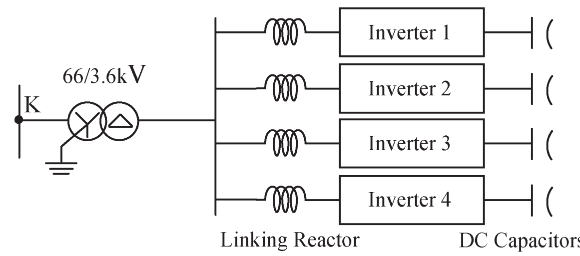

Fig. 5. Schematic diagram of a STATCOM design.

A. SDBR

The concept of the SDBR to augment the FRT capability of the electric generator was first reported in 2004 [37]. The SDBR is used to balance the active power during network disturbance through electrical dissipation. A resistor is dynamically inserted in the generation circuit for a short time during the grid fault, which increases the voltage at the generating end and thus helps in balancing power and electromagnetic torque as well.

In this paper, the SDRB is centrally placed to augment the FRT capability of the wind farm composed of fixed-speed WTGSs, as shown in Fig. 4. There are few ways to implement the switching of the SDBR during the fault condition. In this paper, the SDBR is switched on–off using a standard circuit breaker, which is simple to implement, but on–off conditions may lead to a limit cycle. However, a soft switching scheme can easily be adopted using the insulated gate bipolar transistor (IGBT) or gate turn-off thyristor devices, where the limit cycle issue can be resolved. The wind farm terminal voltage is reasonably chosen as the control input of the centrally placed SDBR, as shown in Fig. 4. During the network fault condition, the wind farm terminal voltage, as well as the voltages at individual wind generators, suddenly reduces. The wind farm voltage is compared with the reference voltage V_{Ref} (in this study, a 0.9 per unit (p.u.) value is considered as reference), and the SDBR is switched on instantly. The essence of the SDBR is that it has a current-squared relationship to the electrical power dissipation, and it quickly restores the wind farm voltage that eventually helps the wind farm to be connected with the power system, fulfilling the FRT requirement of wind farm grid code.

B. STATCOM

Due to the limitation of the state-of-the-art semiconductor switch technology, the power voltage rating is generally around 6.0 kV, with a mainstream switch voltage rating at 4.5 kV. Therefore, in this paper, a three-level inverter-based STATCOM is used to increase the output voltage for suitable connectivity with the wind farm. The STATCOM total rating is considered as 50 MVA. Considering the practical viewpoints and suitability of the simulation analysis, the overall solid-state power circuit combines four three-phase inverter modules, each with a nominal rating of 12.5 MVA, as shown in Fig. 5.

The one-pole structure of a three-level IGBT inverter is shown in Fig. 6(a). The IGBT switching table and control

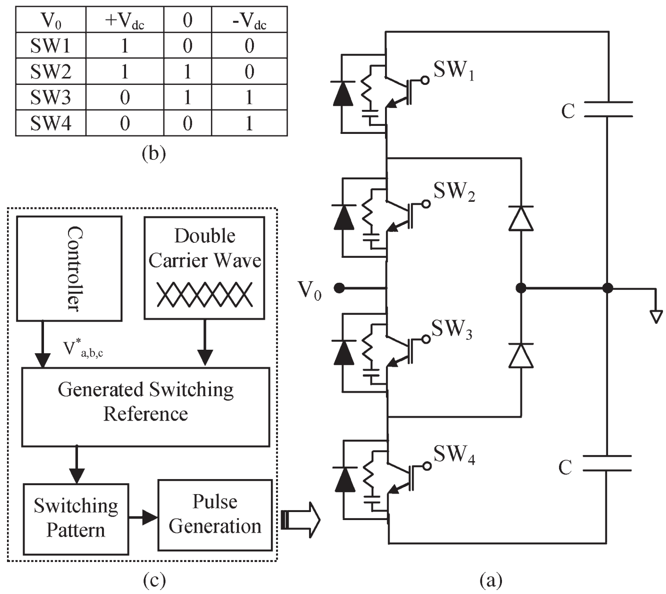

V_0	$+V_{dc}$	0	$-V_{dc}$
SW1	1	0	0
SW2	1	1	0
SW3	0	1	1
SW4	0	0	1

Fig. 6. Schematic diagram of a STATCOM switching circuit. (a) One-pole structure. (b) Switching table. (c) Pulse generation system.

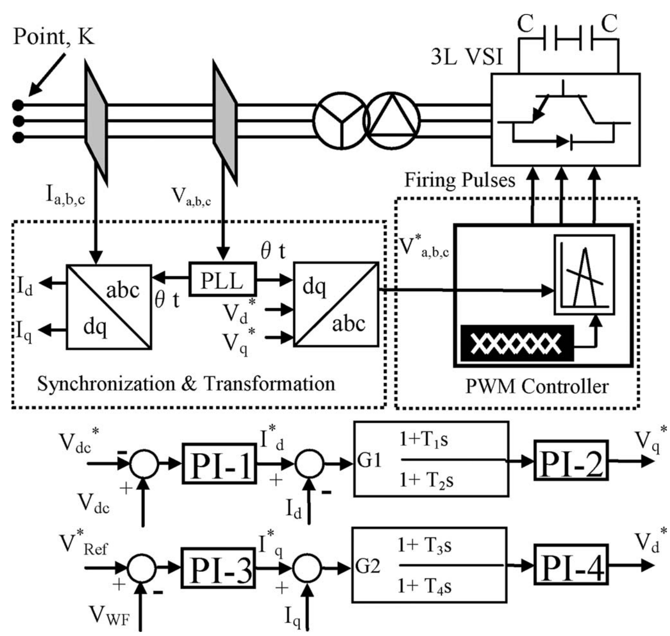

Fig. 7. Control block diagram of a 3L VSI-based STATCOM.

methodology of the STATCOM are shown in Fig. 6(b) and (c), respectively. The aim of the control is to maintain the desired voltage magnitude (V_{Ref2} in Fig. 4) at the wind farm terminal. For the control of the voltage source inverter (VSI), the well-known cascaded vector control scheme is used, as shown in Fig. 7.

C. Pitch Controller

The conventional pitch controller is considered in this study, which progresses the error signal between the wind generator output power and the reference (1.0 p.u.) through a PI controller [6]. The time delay of the servo system is considered as 5 s, and the rate limiter value is chosen as 10°/s.

D. Sizing of the SDBR and STATCOM Considered

One of the objectives of this study is to get some approximate idea about the size of the SDBR and STATCOM required to augment the FRT of a grid-connected wind farm. An earlier study shows that the size of the STATCOM that is required to stabilize a grid-connected wind farm is almost close to the MVA rating of the wind farm itself [22] when only STATCOM is the compensating device used at the generation side. On the other hand, a 1.0 p.u. braking resistor might be sufficient to stabilize the system when only the SDBR is used.

When both the STATCOM and the SDBR are used in the system for stabilizing the wind farm during the grid fault condition, the optimum sizing of the devices also depends on the types and duration of faults and grid code requirements. Therefore, an analytical method may not be appropriate to determine the optimum sizing in this case. In the following section, a detailed simulation study is carried out considering different types of faults, fault duration, wind farm recent grid codes, etc., which will give an idea about the approximate sizing of the SDBR and STATCOM required to stabilize the system.

V. Simulation Analyses

The system shown in Fig. 1 is simulated using the laboratory standard power system simulator PSCAD/EMTDC [33]. FORTRAN program is incorporated with PSCAD to implement the six-mass drive train model of the WTGS. The time step is chosen to be 0.00002 s. The simulation time is chosen to be 5.0 and 600 s for transient and dynamic stability analyses, respectively.

In the simulation study, it is assumed that wind speed is constant and equivalent to the rated speed during transient analysis. This is because it may be considered that wind speed does not change dramatically during the short time interval of the simulation for the transient characteristic analysis. The wind farm grid code is fairly important to analyze the transient characteristics of the WTGS. FRT or low-voltage ride through (LVRT) is now required to be considered for connection of large-scale wind farms in power systems. The FRT complaint that the wind farm must remain connected to the system during network disturbance because a shutdown of large wind farm can have a serious effect on the power system normal operation. In this paper, the simulation results are described in light of the recent grid code, set by E.ON Netz, recently known as TenneT TSO GmbH, as shown briefly in Fig. 8 [10], [11]. Symmetrical three-line-to-ground (3LG) and unsymmetrical double-line-to-ground (2LG), double-line-to-line (2LS), and single-line-to-ground (1LG) faults are considered for transient analysis. Simulation analyses are described in the following sections.

A. Transient Analysis Using a Lumped Model of the WTGS Considering Only the SDBR

In this case, a one-mass lumped model is used as the drive train of a fixed-speed WTGS, and the transient effect of the SDBR is demonstrated considering a 100-ms 3LG fault. First, a 1.0 p.u. (based on the system base) SDBR is inserted at the wind farm terminal, and the responses of voltages at different

This article has been accepted for inclusion in a future issue of this journal. Content is final as presented, with the exception of pagination.

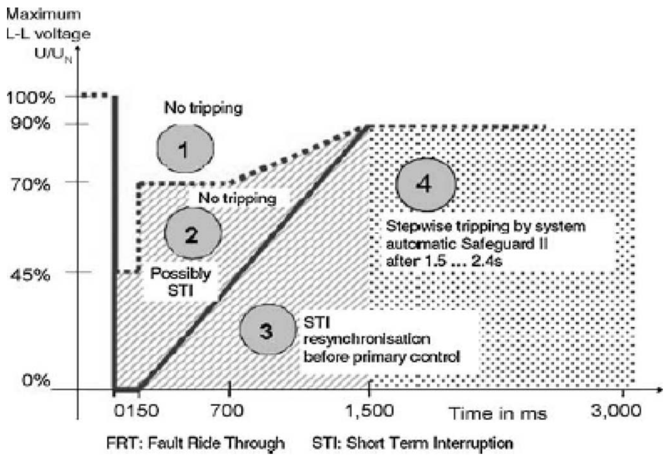

Fig. 8. LVRT standard set by E.ON Netz.

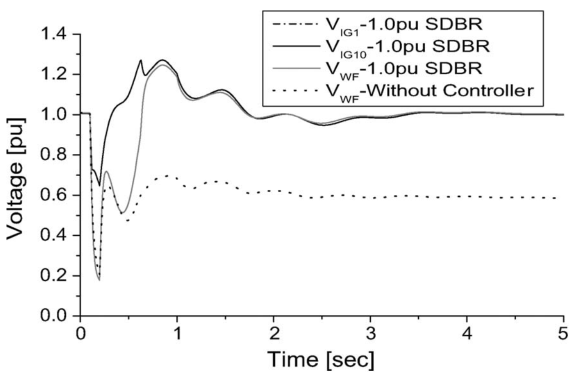

Fig. 9. Voltage responses (100-ms fault, one mass, 3LG).

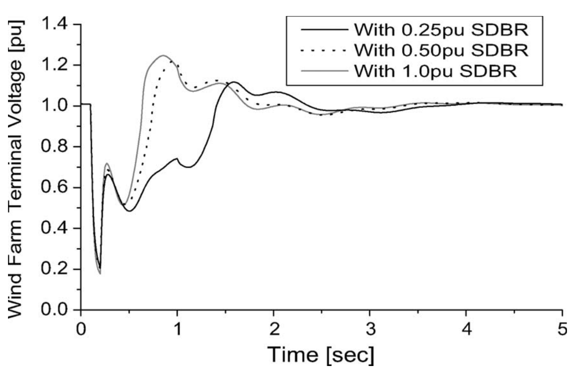

Fig. 10. Voltage responses with different values of SDBR (100-ms fault, one mass, 3LG).

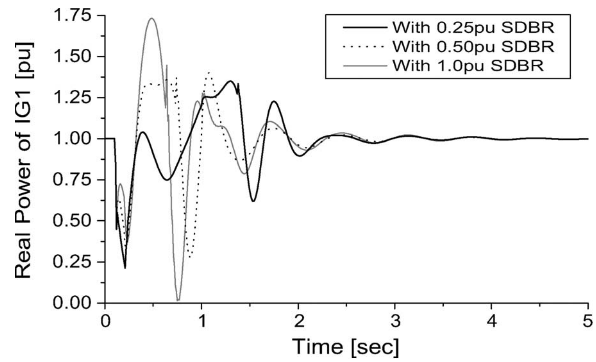

Fig. 11. Real power of IG-1 with different values of SDBR (100-ms fault, one mass, 3LG).

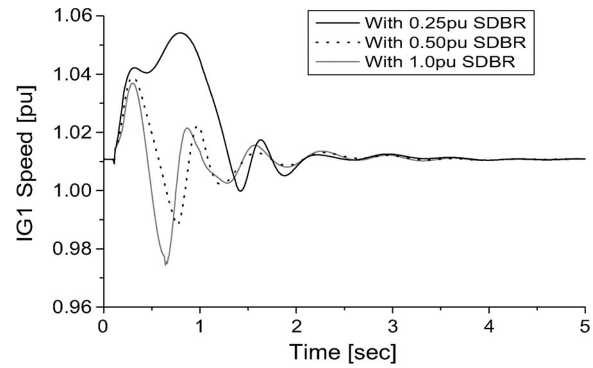

Fig. 12. Rotor speed of IG-1 with different values of SDBR (100-ms fault, one mass, 3LG).

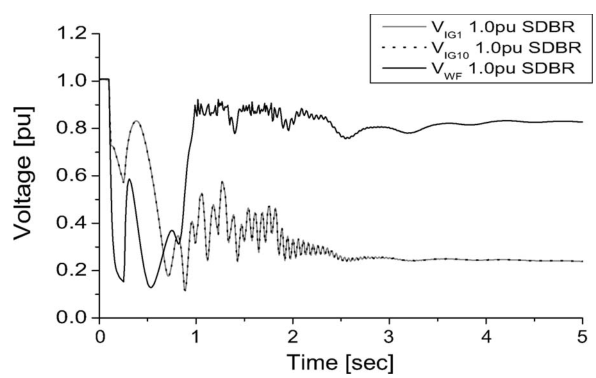

Fig. 13. Voltage responses with different values of SDBR (150-ms fault, 3LG).

wind generators and wind farm terminals are shown in Fig. 9. Fig. 9 presents the expected result that the FRT is not possible unless the SDBR or other compensative tools are considered. Voltage responses with a 1.0 p.u. SDBR and reduced values of the SDBR are shown in Fig. 10. Using the same values, the real power and IG rotor speed responses for WTGS-1 are shown in Figs. 11 and 12, respectively. From Fig. 11, it is shown that a too large value of the SDBR may cause overloading of the wind generator, and a too small value delays the voltage recovery shown in Fig. 10. In this analysis, a 0.25 p.u. SDBR is found to be optimum to augment the FRT of the wind generator considering a one-mass lump model. However, for a longer duration fault (150 ms), the system is found to be unstable even with a 1.0 p.u. SDBR, as shown in Fig. 13. One possible reason might be that GOV control of the SG is not sufficient enough to survive against a longer duration fault without an additional compensating device, which may have some impact on the overall system. In addition, the IG may require some reactive power support to reestablish its electromagnetic torque quickly during a longer fault condition.

B. Transient Analysis Using a Six-Mass Drive Train of the WTGS Considering Only the SDBR

In this case, a six-mass drive train model of the fixed-speed WTGS is used, and the transient effect of the SDBR is analyzed considering both 100- and 150-ms 3LG faults. The terminal

This article has been accepted for inclusion in a future issue of this journal. Content is final as presented, with the exception of pagination.

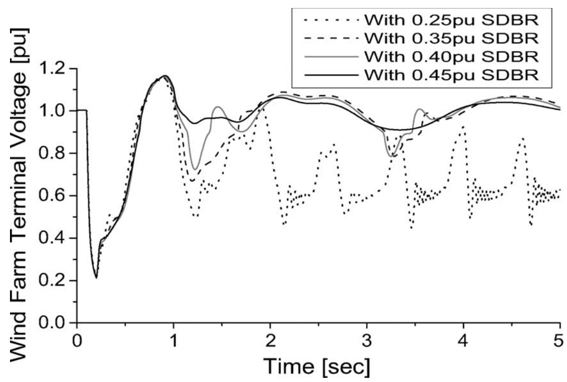

Fig. 14. Voltage responses with different values of SDBR (100-ms fault, multimass, 3LG).

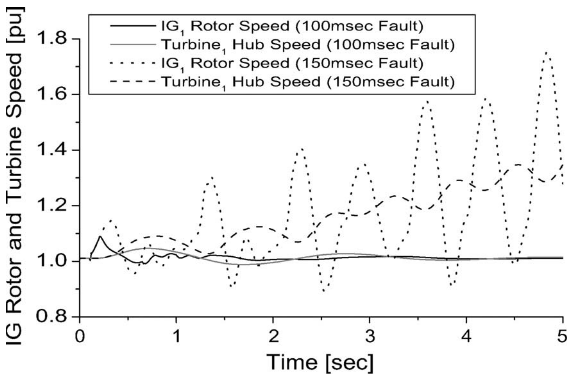

Fig. 15. IG rotor and turbine hub speed of WTGS-1 with an SDBR value of 0.45 p.u. (100- and 150-ms faults, multimass, 3LG).

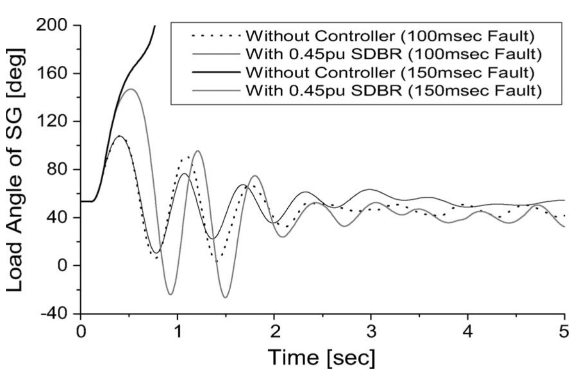

Fig. 16. Load angle of the SG (100- and 150-ms faults, multimass, 3LG).

voltage of the wind farm for different values of the SDBR are shown in Fig. 14 for the fault with 100 ms. It is shown that the SDBR with a 0.25 p.u. value is not sufficient to achieve FRT when a six-mass model is considered. At a 0.45 p.u. SDBR, the system is found to be stable with a 100-ms 3LG fault. The IG rotor and turbine speed of WTGS-1 are shown together in Fig. 15 using a 0.45 p.u. SDBR for both 100- and 150-ms faults, and the WTGS is found to be unstable for a longer fault duration. The SG becomes quickly stable, as shown in Fig. 16, for both 100- and 150-ms faults, although the SG is found to be unstable for a longer fault duration when the SDBR is not considered. The power and energy dissipated by the 0.45 p.u. SDBR are shown in Fig. 17. It is needed to mention that the low-speed shaft stiffness of the six-mass drive train

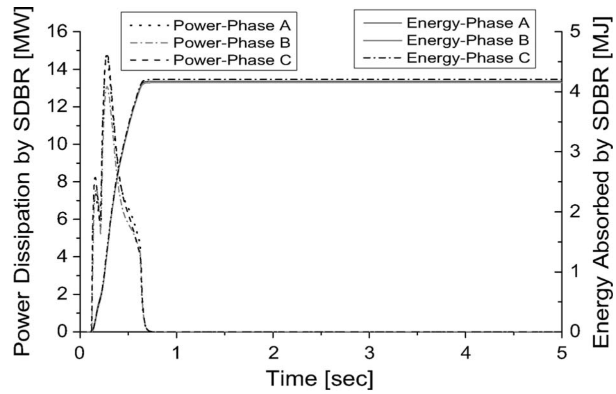

Fig. 17. Power and energy dissipated by the SDBR (100-ms fault, multimass, 3LG).

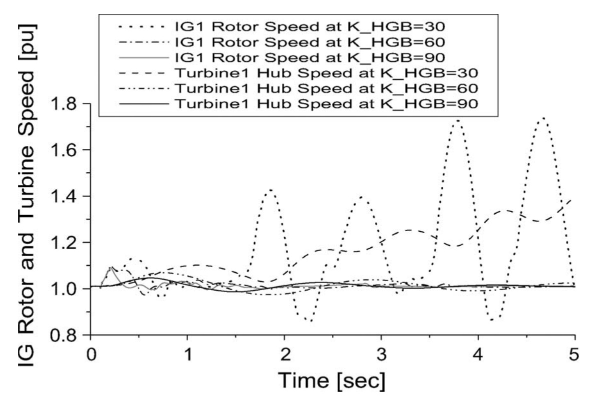

Fig. 18. Effect of shaft stiffness on fault analysis (100-ms fault, multimass, 3LG).

model has a significant effect on the fault analysis of the fixed-speed WTGS. This is because the torque stress on the shaft has a direct influence on stiffness and rotational speed, as reported in [6]. The turbine and generator rotor speed oscillations considering different values of shaft stiffness are demonstrated in Fig. 18.

Therefore, it is needed to consider a multimass drive train model of the WTGS for the fault analysis using the SDBR. In addition, it may be difficult to achieve the FRT of a power-system-connected wind farm as per grid code, particularly in the case of a longer fault duration, using SDBR only.

C. Transient Analysis With the SDBR and STATCOM

Here, extensive simulation analysis is presented using different values of the SDBR and the STATCOM to determine the minimum value of the proposed system that is sufficient to augment the FRT of the wind farm, as described below.

1) SDBR and 50 MVA STATCOM: First, a 3LG fault of 150 ms is considered to occur at the fault point F of the model system shown in Fig. 1. The STATCOM rating is considered same as the wind farm rating, i.e., 50 MVA. The terminal voltage of the wind farm with a 50 MVA STATCOM and different values of the SDBR are shown in Fig. 19. It is shown that using only a 50 MVA STATCOM is sufficient to overcome the 150-ms fault and meet the grid code requirement. The 50 MVA STATCOM along with a 0.45 p.u. SDBR and a

This article has been accepted for inclusion in a future issue of this journal. Content is final as presented, with the exception of pagination.

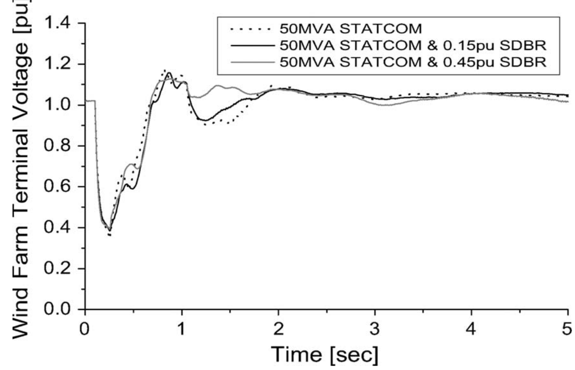

Fig. 19. Voltage responses with a 50 MVA STATCOM and different values of the SDBR (150-ms fault, multimass, 3LG).

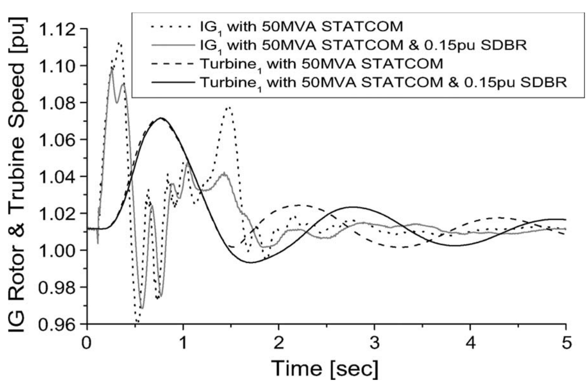

Fig. 20. IG rotor and turbine speed of WTGS-1 with a 50 MVA STATCOM and different values of the SDBR (150-ms fault, multimass, 3LG).

reduced 0.15 p.u. SDBR can augment the FRT better than using only STATCOM. The IG rotor speed and turbine speed of WTGS-1 shown in Fig. 20 also validates the effectiveness of the combined use of STATCOM and SDBR. However, incorporation of a 50 MVA STATCOM increases the total investment cost of the overall system, which can be reduced by minimizing the size of the STATCOM unit and finding the suitable size of the SDBR unit.

2) SDBR and 12.5 MVA STATCOM: In this analysis, the three inverter modules of the STATCOM shown in Fig. 5 are switched off, and therefore, a 125 MVA STATCOM is in service. The SDBR value is kept constant at 0.45 p.u., and a 3LG fault with 100 and 150 ms is considered. The response of the wind farm terminal voltage is shown in Fig. 21. The load angle response of the SG is also shown in Fig. 22. It can be said that integration of a small STATCOM with a 0.45 p.u. SDBR cannot augment the FRT capability of the wind farm as per grid code shown in Fig. 8 for a 150-ms fault, although it shows a better FRT characteristic than using only a 0.45 p.u. SDBR, as shown in Figs. 14 and 21, in the case of a 100-ms fault. The transient stability improvement of the SG is also not evident for a longer fault duration, in this case, as shown in Figs. 16 and 22.

3) SDBR and 25 MVA STATCOM: In this analysis, the two inverter modules of the STATCOM shown in Fig. 5 is switched off, and therefore, a 25 MVA STATCOM is in service. A wind farm terminal voltage with a 25 MVA STATCOM and different

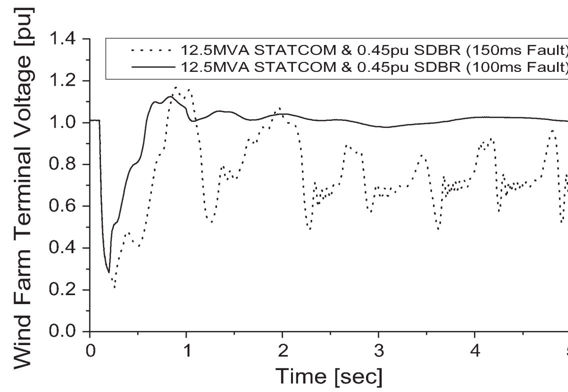

Fig. 21. Voltage responses with a 12.5 MVA STATCOM and 0.45 p.u. SDBR (100- and 150-ms faults, multimass, 3LG).

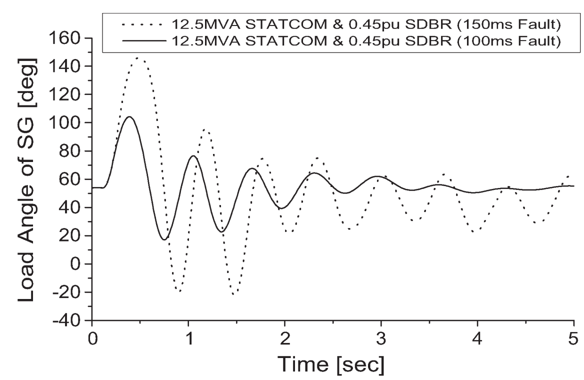

Fig. 22. Load angle of the SG with a 12.5 MVA STATCOM and a 0.45 p.u. SDBR (100- and 150-ms faults, multimass, 3LG).

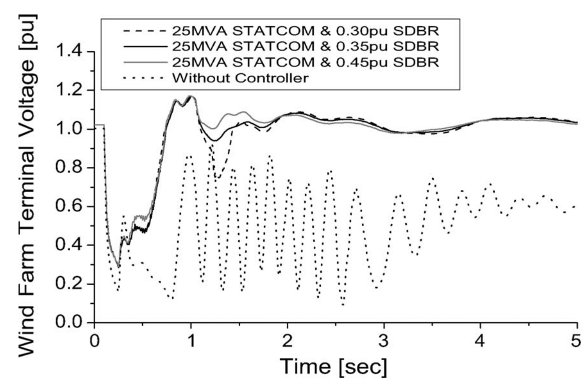

Fig. 23. Voltage responses with a 25 MVA STATCOM and different values of the SDBR (150-ms fault, multimass, 3LG).

values of the SDBR are shown in Fig. 23, considering a 150-ms 3LG fault. The responses of the IG rotor and turbine speed of WTGS-1 are shown in Fig. 24. It is shown that a 0.35 p.u. SDBR along with a 25 MVA STATCOM gives a sufficient FRT improvement of the wind farm that also satisfies the grid code. Therefore, this combination is used as the base case for the rest of the analysis in this study. The responses of the reactive power and the dc-link voltage of the STATCOM are shown in Figs. 25 and 26, respectively. It is found that the transient stability of the SG significantly improves using this combination, as shown in Fig. 27.

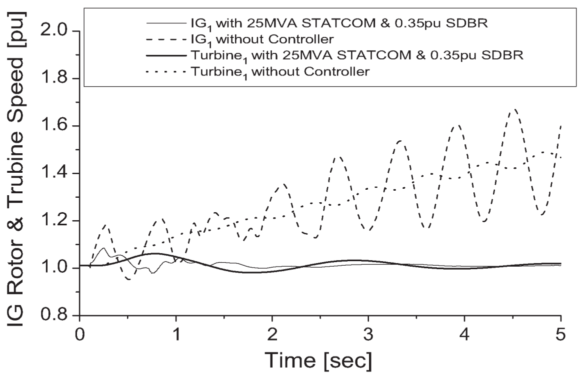

Fig. 24. IG rotor and turbine speed of WTGS-1 with a 25 MVA STATCOM and a 0.35 p.u. SDBR (150-ms fault, multimass, 3LG).

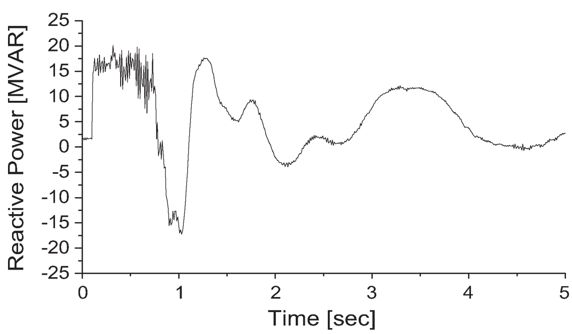

Fig. 25. Reactive power of a STATCOM (150-ms fault, multimass, 3LG).

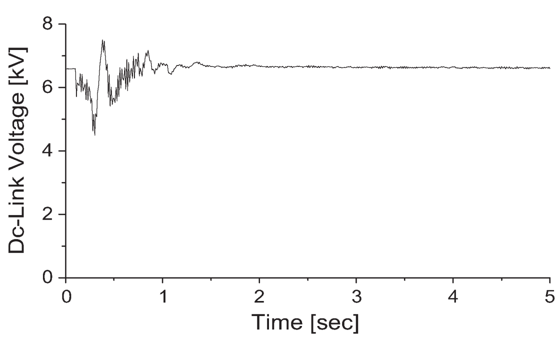

Fig. 26. DC-link voltage of a STATCOM (150-ms fault, multimass, 3LG).

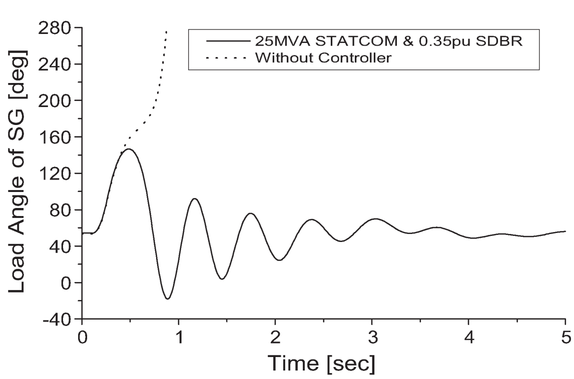

Fig. 27. Load angle of the SG with a 25 MVA STATCOM and a 0.35 p.u. SDBR (150-ms fault, multimass, 3LG).

D. Unsymmetrical Fault Analysis

Using the combination of a reduced 0.35 p.u. SDBR and a 25 MVA STATCOM, the FRT of the wind farm for 150 duration

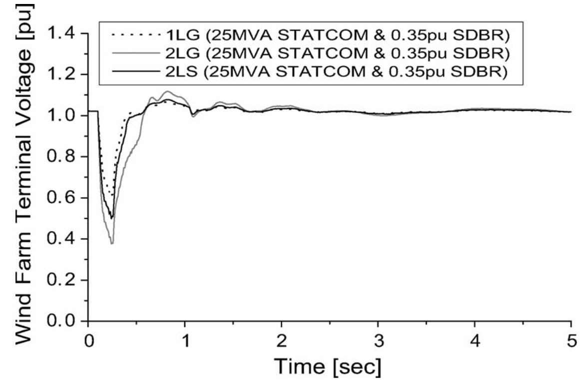

Fig. 28. Voltage responses with a 25 MVA STATCOM and a 0.35 p.u. SDBR (150-ms fault, multimass, 2LG, 2LS, 1LG).

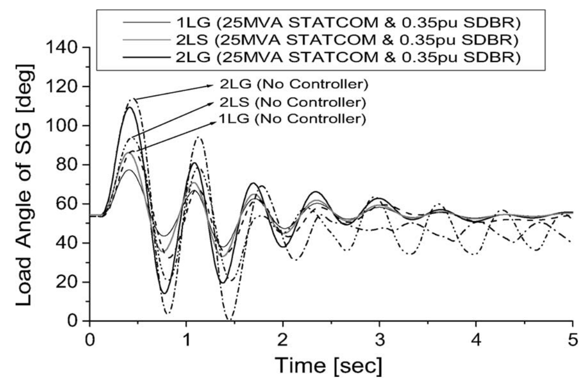

Fig. 29. Load angle of the SG with a 25 MVA STATCOM and a 0.35 p.u. SDBR (150-ms fault, multimass, 2LG, 2LS, 1LG).

unsymmetrical faults is analyzed. The responses of wind farm terminal voltages for 2LG, 2LS, and 1LG faults are shown in Fig. 28. From this figure, it can be understood that a 0.35 p.u. SDBR and a 25 MVA STATCOM even augment the wind farm FRT capability for unsymmetrical faults. The improvement of transient stability of the SG is also evident for this combination, as shown in Fig. 29.

E. Blade–Shaft Torsional Oscillation Reduction of the WTGS

In this analysis, we can observe how much the blade–shaft torsional oscillations of the fixed-speed WTGS can be reduced using the proposed 0.35 p.u. SDBR and 25 MVA STATCOM when symmetrical 3LG fault occurs in the power system. The high-speed side of the shaft between the generator and the gearbox is relatively stiff compared with the low-speed side of the shaft between the gearbox and the turbine hub. The eigenfrequency of the high-speed shaft is about 30–40 Hz. On the other hand, the low-speed shaft natural frequency is about 2–3 Hz [36]. The symmetrical and unsymmetrical faults cause 50- and 100-Hz torque oscillations, respectively, in the IG of the fixed-speed WTGS [6]. Due to the high stiffness of the shaft between the generator and the gearbox, this oscillation is expected to be reached at the gearbox. Therefore, proper care should be taken to damp out the torque oscillations.

The return maps of the high-speed shaft torque, low-speed shaft torque, and torque between the hub and the blade with and without considering the proposed scheme are shown in

This article has been accepted for inclusion in a future issue of this journal. Content is final as presented, with the exception of pagination.

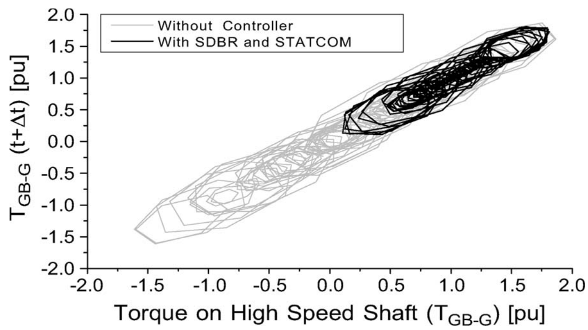

Fig. 30. Return map for the high-speed shaft torque (3LG).

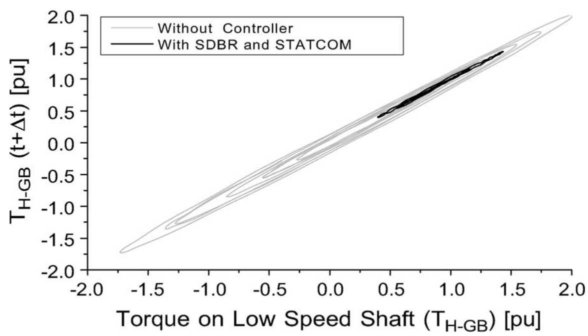

Fig. 31. Return map for the low-speed shaft torque (3LG).

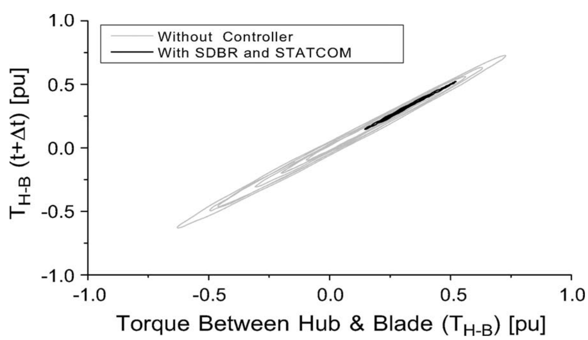

Fig. 32. Return map for the torque between the hub and blade-1 (3LG).

Figs. 30–32, respectively, for WTGS-1 of the wind farm. It is found that the proposed scheme can reduce well the blade–shaft torsional oscillations of the fixed-speed WTGS. It is expected that a 50-Hz torque oscillation will be transmitted to the high-speed shaft, as can be also understood from Fig. 30. Due to the relatively high spring constant of the high-speed shaft, those oscillations reach to the gearbox, and then, it is damped out, as shown in Figs. 31 and 32, when the SDBR and the STATCOM are used together.

F. Dynamic Analysis

Real wind speed data measured at the Hokkaido Island, Japan, is used in different WTGSs of the wind farm, as shown in Fig. 33. It is seen that using the reduced value of the STATCOM can even compensate the reactive power demand of the wind farm terminal during normal operation and therefore can maintain the terminal voltage at the desired level set by transmission system operators, as shown in Fig. 34.

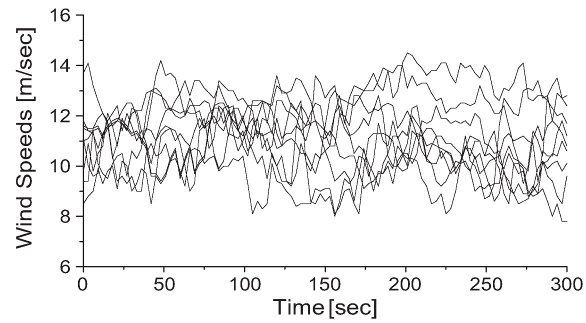

Fig. 33. Wind speed data.

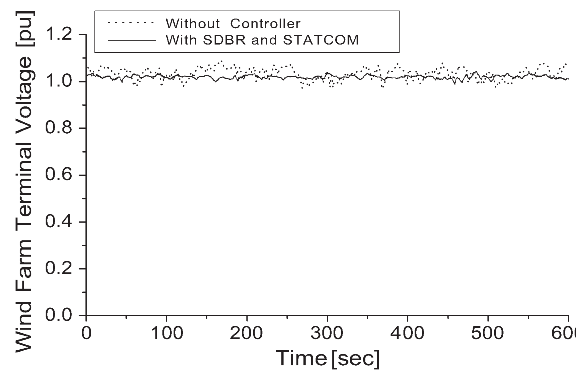

Fig. 34. Wind farm terminal voltage at randomly varying wind speed.

TABLE II
DRIVE TRAIN PARAMETERS

Inertia Constants		Spring Constants	
$H_{B(1,2,3)}$	0.95	$K_{HB(1,2,3)}$	1259.8
H_H	0.02	K_{HGB}	60.0
H_{GB}	0.13	K_{GBG}	1834.1
H_G	0.30		

VI. CONCLUSION

This paper has focused on the transient and dynamic stability augmentation of a grid-connected wind farm composed of fixed-speed WTGSs using a combination of the SDBR and the STATCOM in a cost-effective proportion. From the extensive simulation analyses, it is found that a 0.3–0.35 p.u. SDBR (based on the system base) and a 20–25 MVA STATCOM (40%–50% of the wind farm capacity) is a good proportion to stabilize the transient and dynamic stabilities of the wind farm. This proportion is considered for analyzing all types of symmetrical and unsymmetrical fault conditions, and it is found that the wind farm FRT requirement is fulfilled as per recent grid code. It is also investigated that this proportion can significantly minimize the blade–shaft oscillation of the fixed-speed WTGS, which is one of the important observations from this study. Through the extensive simulation analysis, few more relevant observations are given below for further study on the SDBR and the STATCOM for stability augmentation of grid-connected wind generators.

1) It was found that only the SDBR may not fulfill the FRT requirement of the wind farm as per recent grid code when it is connected to the power grid, particularly for a longer duration of a fault case scenario. The other generators available in the power system may have some

pessimistic impact during the FRT of the wind farm for a longer duration fault as the braking resistor is dynamically inserted in series in this configuration.

2) To precisely determine the size of the SDBR that is inserted at the terminal of the wind farm composed of fixed-speed WTGSs, a multimass drive train model should be considered in the analysis.
3) A pertinent proportion of the SDBR and the STATCOM is eventually related to active and reactive power balance, and thus, special attention should be given to determine the size of the SDBR and the STATCOM to augment dynamic and transient stability of a power-system-connected wind farm.

Finally, it is concluded that if the capacity of the SDBR and the STATCOM can be chosen properly, the combination will be a cost-effective means to augment the dynamic and transient stability of a grid-connected wind farm composed of fixed-speed WTGSs.

APPENDIX

The six- and three-mass drive train parameters in per unit based on high-speed rotation are shown in Table II [6], [36].

REFERENCES

[1] GWEC publications, Global Wind 2010 Report, The Global Wind Energy Council. [Online]. Available: http://www.gwec.net/

[2] A. Sumper, O. G. Bellmunt, A. S. Andreu, R. V. Robles, and J. R. Duran, "Response of fixed speed wind turbines to system frequency disturbances," *IEEE Trans. Power Syst.*, vol. 24, no. 1, pp. 181–192, Feb. 2009.

[3] C. L. Souza, L. M. Neto, G. C. Guimaraes, and A. J. Moraes, "Power system transient stability analysis including synchronous and induction generator," in *Proc. IEEE Porto Power Tech.*, 2001, vol. 2, p. 6.

[4] J. Tamura, T. Yamazaki, M. Ueno, Y. Matsumura, and S. Kimoto, "Transient stability simulation of power system including wind generator by PSCAD/EMTDC," in *Proc. IEEE Porto Power Tech.*, 2001, vol. 4, EMT-108, doi:10.1109/PTC.2001.964821.

[5] E. S. Abdin and W. Xu, "Control design and dynamic performance analysis of a wind turbine-induction generator unit," *IEEE Trans. Energy Convers.*, vol. 15, no. 1, pp. 91–96, Mar. 2000.

[6] S. M. Muyeen, J. Tamura, and T. Murata, *Stability Augmentation of a Grid-connected Wind Farm*. London, U.K.: Springer-Verlag, Oct. 2008.

[7] R. Zavadil, N. Miller, A. Ellis, and E. Muljadi, "Making connections [wind generation facilities]," *IEEE Power Energy Mag.*, vol. 3, no. 6, pp. 26–37, Nov./Dec. 2005.

[8] Federal Energy Regulatory Commission (FERC), United States of America, Docket No. RM05-4-000 - Order No. 661, Interconnection for Wind Energy, Jun. 2, 2005.

[9] Wind Farm Power Station Grid Code Provisions, WFPS1, pp. 213–216, Jan. 2007.

[10] E.On Netz, Grid Code, High- and Extra-High Voltage, Apr. 2006. [Online]. Available: www.eon-netz.com/

[11] B. Singh and S. N. Singh, "Wind power interconnection into the power system: A review of grid code requirements," *Elect. J.*, vol. 22, no. 5, pp. 54–63, Jun. 2009.

[12] T. Kinjo, T. Senjyu, N. Urasaki, and H. Fujita, "Output levelling of renewable energy by electric double-layer capacitor applied for energy storage system," *IEEE Trans. Energy Convers.*, vol. 21, no. 1, pp. 221–227, Mar. 2006.

[13] S. M. Muyeen, R. Takahashi, M. H. Ali, T. Murata, and J. Tamura, "Transient stability augmentation of power system including wind farms by using ECS," *IEEE Trans. Power Syst.*, vol. 23, no. 3, pp. 1179–1187, Aug. 2008.

[14] L. Zhang, C. Shen, M. L. Crow, L. Dong, S. Pekarek, and S. Atcitty, "Performance indices for the dynamic performance of FACTS and FACTS with energy storage," *Elect. Power Compon. Syst.*, vol. 33, no. 3, pp. 299–314, Mar. 2005.

[15] S. W. Mohod and M. V. Aware, "Micro wind power generator with battery energy storage for critical load," *IEEE Syst. J.*, vol. 6, no. 1, pp. 118–125, Mar. 2012.

[16] H. Takabayashi, S. Sano, Y. Hirose, K. Mitani, and H. Wakatabe, "The application of valve-regulated lead acid batteries to wind power generation system," in *Proc. 31st Int. Telecommun. Energy Conf.*, Incheon, Korea, 2009, pp. 1–5.

[17] S. C. Tripathy, M. Kalantar, and R. Balasubramanian, "Dynamics and stability of wind and diesel turbine generators with superconducting magnetic energy storage on an isolated power system," *IEEE Trans. Energy Convers.*, vol. 6, no. 4, pp. 579–585, Dec. 1991.

[18] S. Nomura, Y. Ohata, T. Hagita, H. Tsutsui, S. Tsuji-Iio, and R. Shimada, "Wind farms linked by SMES systems," *IEEE Trans. Appl. Supercond.*, vol. 15, no. 2, pp. 1951–1954, Jun. 2005.

[19] S.-S. Chen, L. Wang, W.-J. Lee, and Z. Chen, "Power flow control and damping enhancement of a large wind farm using a superconducting magnetic energy storage unit," *IET Renew. Power Gener.*, vol. 3, no. 1, pp. 23–38, Mar. 2009.

[20] F. Islam, H. Hasanien, A. Al-Durra, and S. M. Muyeen, "A new control strategy for smoothing of wind farm output using short-term ahead wind speed prediction and flywheel energy storage system," in *Proc. Amer. Control Conf.*, Montreal, QC, Canada, Jun. 2012, pp. 3026–3031.

[21] S. W. Mohod and M. V. Aware, "A STATCOM-Control scheme for grid connected wind energy system for power quality improvement," *IEEE Syst. J.*, vol. 4, no. 3, pp. 346–352, Sep. 2010, Member, IEEE.

[22] S. M. Muyeen, M. A. Mannan, M. H. Ali, R. Takahashi, T. Murata, and J. Tamura, "Stabilization of wind turbine generator system by STATCOM," *IEEJ Trans. Power Energy*, vol. 126-B, no. 10, pp. 1073–1082, 2006.

[23] M. Aten, J. Martinez, and P. J. Cartwright, "Fault recovery of a wind farm with fixed speed induction generators using a STATCOM," *Wind Eng.*, vol. 29, no. 4, pp. 365–375, Jun. 2005.

[24] P. M. Anderson and A. Bose, "Stability simulation of wind turbine systems," *IEEE Trans. Power App. Syst.*, vol. PAS-102, no. 12, pp. 3791–3795, Dec. 1983.

[25] S. M. Muyeen, M. H. Ali, R. Takahashi, T. Murata, and J. Tamura, "Transient stability enhancement of wind generator by a new logical pitch controller," *IEEJ Trans. Power Energy*, vol. 126, no. 8, pp. 742–752, Aug. 2006.

[26] W. Freitas, A. Morelato, and W. Xu, "Improvement of induction generator stability using braking resistors," *IEEE Trans. Power Syst.*, vol. 19, no. 2, pp. 1247–1249, May 2004.

[27] A. Arulampalam, M. Barnes, N. Jenkins, and J. B. Ekanayake, "Power quality and stability improvement of a wind farm using STATCOM supported with hybrid battery energy storage," *IEE Proc.-Gener. Transmiss. Distrib.*, vol. 153, no. 6, p. 701–110, Nov. 2006.

[28] X. Wu, A. Arulampalam, C. Zhan, and N. Jenkins, "Application of a static reactive power compensator (STATCOM) and a dynamic braking resistor (DBR) for the stability enhancement of a large wind farm," *Wind Eng.*, vol. 27, no. 2, pp. 93–106, Mar. 2003.

[29] A. Causebrook, D. J. Atkinson, and A. G. Jack, "Fault ride-through: Shifting the balance of power from blade to electrical resistance," in *Proc. Eur. Wind Energy Conf.*, Athens, Greece, 2006.

[30] A. Causebrook, D. J. Atkinson, and A. G. Jack, "Fault ride-through of large wind farms using series dynamic braking resistors (March 2007)," *IEEE Trans. Power Syst.*, vol. 22, no. 3, pp. 966–975, Aug. 2007.

[31] Y. Wei, L. Hong, Q. Jiang, and Z. Wang, "A new dynamic strategy for improved ride-through capability of wind turbine generator," in *Proc. IEEE Power Energy Soc. Gen. Meet.*, Detroit, MI, USA, 2011, pp. 1–6.

[32] A. M. Hasan and B. Wu, "Comparison among stabilization methods of fixed-speed wind generator system," in *IEEE Energy Conversion Congress and Exposition, ECCE09*, San Jose, CA, USA, Sep. 2009, pp. 2667–2674.

[33] *PSCAD/EMTDC Manual*, Manitoba HVDC Research Center, Winnipeg, MB Canada, 1994.

[34] Heier, *Grid Integration of Wind Energy Conversion System*. Chichester, U.K.: Wiley, 1998.

[35] O. Wasynczuk, D. T. Man, and J. P. Sullivan, "Dynamic behavior of a class of wind turbine generator during random wind fluctuations," *IEEE Trans. Power App. Syst.*, vol. PAS-100, no. 6, pp. 2845–2873, Jun. 1981.

[36] S. A. Papathanassiou and M. P. Papadopoulos, "Mechanical stresses in fixed speed wind turbines due to network disturbances," *IEEE Trans. Energy Convers.*, vol. 16, no. 4, pp. 361–367, Dec. 2001.

[37] A. Causebrook, "Dynamic braking of electric generators for fault ride-though control," U.K. Patent Appl. No. GB0526133.4, Dec. 22, 2005, Newcastle Univ., Newcastle upon Tyne.

S. M. Muyeen (S'03–M'08–SM'12) received the B.Sc. Eng. degree from Rajshahi University of Engineering and Technology (formerly Rajshahi Institute of Technology), Rajshahi, Bangladesh, in 2000 and the M.Sc. Eng. and Dr. Eng. degrees from Kitami Institute of Technology, Kitami, Japan, in 2005 and 2008, respectively, all in electrical and electronic engineering. His Ph.D. research work focused on wind farm stabilization from the viewpoint of low-voltage ride through and frequency fluctuation.

After completing his Ph.D. program, he worked as a Postdoctoral Research Fellow under the versatile banner of the Japan Society for the Promotion of Science from 2008 to 2010 at the Kitami Institute of Technology. He is currently an Assistant Professor with the Electrical Engineering Department, The Petroleum Institute, Abu Dhabi, UAE. He has published over 100 international papers. He has published four books as an author or Editor. His research interests are power system stability and control, electrical machines, flexible alternating current transmission systems, energy storage systems, renewable energy, and high-voltage direct current systems.